

LETTER TO THE EDITOR

Kolmogorov analysis of pulsar TOAN. Galikyan^{1,2}, A.A.Kocharyan³, and V.G. Gurzadyan^{1,4,★}¹ Center for Cosmology and Astrophysics, Alikhanian National Laboratory and Yerevan State University, Yerevan, Armenia² Department of Physics, Sapienza University of Rome, Rome, Italy³ School of Physics and Astronomy, Monash University, Clayton, Australia⁴ SIA, Sapienza University of Rome, Rome, Italy

Received XXX; accepted ZZZ

ABSTRACT

The Kolmogorov stochasticity parameter (KSP) as a sensitive descriptor of degree of randomness of signals is used to analyze the properties of the NANOGrav pulsar timing data associated to a stochastic gravitational wave background. The time of arrival (TOA) data of white noise for 68 pulsars are analyzed regarding their KSP properties. The analysis enables to obtain the degree of randomness of the white noise for various pulsars and to reveal its inhomogeneity, i.e. pulsars with low and high randomness of the white noise. The time-dependence of the randomness in the white noise is also studied, indicating the existence of non-stationary physical processes influencing the pulsar timing. The KSP thus is acting as an indicator for the degree of the agreement between the observations and the timing models and as a test in revealing the contribution of various physical processes in the stochastic background signal.

1. Introduction

The data on the pulsar-timing monitoring obtained by the North American Nanohertz Observatory for Gravitational Waves (NANOGrav) (Agazie, et al 2023a, 2025) and other collaborations opened a new important window to trace variety of processes ongoing in the Universe. The released pulsar timing array (PTA) data are linked to the stochastic gravitational-wave background (GWB) in nanohertz band produced by binary supermassive black holes (Sesana, et al 2008; Agarwal, et al 2023; Sesana and Figeroa 2025), and are also used to constrain bunch of the models such as on the nature of the dark matter, on the evolution of the early cosmology, e.g. (Tiruvaskar and Gordon 2025; Ben-Dayan et al 2025) and refs therein.

The key issue in the pulsar timing is the analysis of the stochastic properties of the time of arrival (TOA) data of residuals for the studied 68 pulsars, e.g. the differences between the observed data and modeled parameters (Lam, et al 2025). Therefore, the study of tiny properties of the stochastic background by different methods and hence, of the residuals' association to the white noise, can be crucial both for revealing the details from the pulsar astrometric parameters of pulsars up those of the supermassive black hole binaries (e.g. of their orbital eccentricities) or of the contribution of other effects, see (Fiscella, et al 2025) and refs therein. Moreover, the white noise can contain the contributions of the instrumental noise, of calibration of the radio telescopes, up to the interference from terrestrial sources. Thus, while the comprehensive study of the white noise is crucial for the revealing of the origin of the nanohertz gravitational wave background, the use of different descriptors can be of particular importance for separation of contributions of the mentioned or other effects in the white noise.

In this study we apply the Kolmogorov stochasticity parameter (KSP) to analyse the properties of the white noise (cf.(Barenboim, et al 2025)) of TOA associated both to the TOA data and the pulsar timing models. The Kolmogorov stochasticity parameter is a sensitive quantitative descriptor of the de-

gree of randomness of sequences (Kolmogorov 1933; Arnold 2008a). The KSP has been applied to the analysis of various signals (e.g. (Arnold 2008a; Atto, et al 2013; Hoffman, et al 2023), including of human genomic sequences (Gurzadyan, et al 2015), as well as of astrophysical origin (Gurzadyan and Kocharyan 2008; Gurzadyan, et al 2009, 2010; Gurzadyan, Durret 2011; Galikyan, et al 2025), see also (Gurzadyan 1999). For example, the KSP enabled to trace the properties of the Cold Spot as of a non-Gaussian region in the Cosmic microwave background sky (*Planck* data) and to conclude on its void origin in the large scale matter distribution (Gurzadyan, et al 2014); the void nature of the Cold Spot was soon after confirmed by an galaxy survey study (Szapudi, et al 2015).

Thus, we use the KSP, (a) to quantify how independent are the TOA residuals, (b) to reveal how much homogeneous is the randomness regarding to individual pulsars, i.e. if there are pulsars attributed to low and high randomness signals, (c) to test if non-stationary effects can be traced in the white noise, (d) to determine how closely the timing models for individual pulsars match their observations.

2. Kolmogorov stochasticity parameter**2.1. Theoretical and Empirical Cumulative Distribution Functions**

First, let us define the Kolmogorov stochasticity parameter as in (Kolmogorov 1933; Arnold 2008a,b,c, 2009a,b). Let X be a real-valued random variable. Its cumulative distribution function (CDF) is

$$F(x) \equiv \Pr(X \leq x), \quad (1)$$

where $\Pr(\cdot)$ denotes probability under the assumed probabilistic model. Throughout this section, F will be referred to as the *theoretical (model/null) CDF*.

Given an observed sample x_1, \dots, x_n (not necessarily distinct), let $x_{(1)} \leq x_{(2)} \leq \dots \leq x_{(n)}$ denote the order statistics. The

★ Email: gurzadyan@yerphi.am

corresponding *empirical CDF (ECDF)* is defined by

$$F_n(x) \equiv \frac{1}{n} \sum_{i=1}^n \mathbf{1}\{x_i \leq x\}, \quad (2)$$

which is a right-continuous step function:

$$F_n(x) = \begin{cases} 0, & x < x_{(1)}, \\ k/n, & x_{(k)} \leq x < x_{(k+1)}, \quad k = 1, \dots, n-1, \\ 1, & x_{(n)} \leq x. \end{cases} \quad (3)$$

Our basic goal is to quantify the discrepancy between the ECDF of the data and a reference (theoretical) CDF F . In applications, F represents a null/model hypothesis (e.g., a specified distribution, or a distribution implied by a simulated noise model). When F is fully specified and continuous, the resulting statistic is distribution-free under the null.

2.2. Kolmogorov Distance and Stochasticity Parameter

Define the (one-sample) *Kolmogorov distance*:

$$D_n \equiv \sup_{x \in \mathbb{R}} |F_n(x) - F(x)|, \quad (4)$$

and its scaled form, the *Kolmogorov stochasticity parameter*:

$$\lambda_n \equiv \sqrt{n} D_n = \sqrt{n} \sup_{x \in \mathbb{R}} |F_n(x) - F(x)|. \quad (5)$$

Because the sample $\{X_i\}_{i=1}^n$ is random, the ECDF F_n and thus λ_n are random variables. Under the null hypothesis $H_0 : X_1, \dots, X_n \sim F$ (with F continuous), λ_n has a distribution function

$$\Phi_n(\lambda) \equiv \Pr(\lambda_n \leq \lambda), \quad (6)$$

which converges to a universal limiting distribution $\Phi(\cdot)$ independent of F :

$$\Phi(\lambda) = \sum_{k=-\infty}^{+\infty} (-1)^k e^{-2k^2 \lambda^2}, \quad \Phi(0) = 0. \quad (7)$$

This is the statement of Kolmogorov's theorem (Kolmogorov 1933).

Note that, according to this theorem and the property of the limiting function Φ , the probable values of λ are within 0.3 and 2.2, i.e. at its lower values $\Phi(\lambda)$ tends rapidly to 0 and at higher values to 1, respectively.

An important feature of the KSP criterion is its applicability to relatively small sequences (orbits of dynamical systems) as explicitly is shown in (Arnold 2008a), comparing two sequences of 15 two-digit numbers and concluding that the stochasticity probability of the one sequence is approximately 300 times higher than of the other one. Then, for random sequences, the stochasticity parameter λ_n will have a distribution close to the function $\Phi(\lambda)$, while the distribution will be different from that function for non-random sequences.

The numerical experiments performed in (Gurzadyan, et al 2011) using a single scaling of the ratio of stochastic to regular components of the generated sequences, including of uniform distribution, reveal the efficiency of the KSP as an indicator of the degree of randomness of composite signals.

3. Pulsar timing

Pulsar timing is based on measuring TOAs of radio pulses with high precision and comparing them to the predictions of a timing model. The timing model encodes all deterministic contributions to the TOAs—such as the pulsar's spin evolution, astrometric parameters, binary motion (when present), and propagation effects. Any mismatch between the measured TOAs and the timing model—i.e., the timing residuals—contains information about additional physical or instrumental processes not captured by the deterministic model.

These stochastic contributions are commonly separated into low-frequency, temporally correlated “red noise” (e.g., intrinsic spin noise or a stochastic gravitational-wave background), which are the type of signals that researchers usually look for. It is important to note that not all pulsars exhibit a red-noise component, and the contribution to the red noise can come from various effects (Fiscella, et al 2025), which can introduce characteristic structures in timing residuals. High-frequency, uncorrelated “white noise” arises mainly from radiometer noise and measurement uncertainties, representing random fluctuations in the time series. The white-noise component can be calculated as $\text{WhiteNoise} = \text{TOA} - \text{TimingModel} - \text{RedNoise}$ (if present).

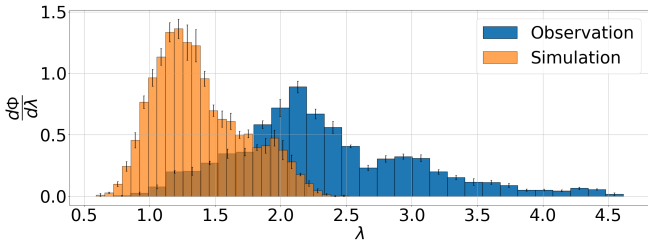
For our analysis, we use PINT (Luo, et al 2019, 2021; Subobhanan, et al 2024), a high-precision open-source package for pulsar timing data analysis written in Python. It is developed in collaboration with NANOGrav and is largely used for analysis (Agazie, et al 2023a,b; Smith, et al 2023), e.t.c. It allows one to read TOA data and load timing models with their parameters, e.g., provided by NANOGrav (NANOGrav 2025). Moreover, in PINT, one can simulate the white and red noise components of pulsar signals separately and estimate the white-noise contribution. The simulated white noise and the observed white noise should have the same statistical properties, i.e. the signal that we are calling white noise in the observed data is indeed a white-noise signal. To test this, we use the KSP as a statistical characteristic of a signal and compare the observed signal with the simulated one as described in 4.1.

4. Analysis

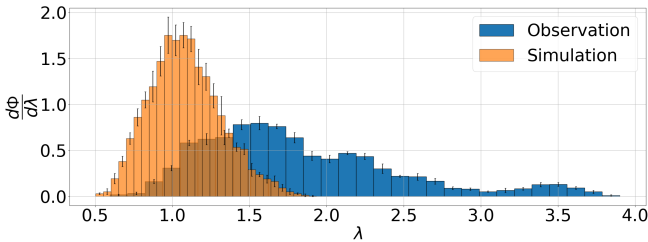
Consider a time series of length N that represents the residual component of the TOAs (NANOGrav 2025). To obtain the KSP characteristic histogram for the series, we calculate λ inside a sliding window of length $10^{-1} \cdot N$ with a sliding step of $10^{-3} \cdot N$. Inside the window, we randomly select 80% of the points and calculate λ using the generalized normal distribution as the theoretical distribution. Its probability density is given via Eq.(8). The final λ for that window is the mean of the 80% repeated 5 times. Namely, the algorithm estimates the distribution of λ , then its running 4 more times allows to estimate the λ distribution's stability, as the 80% subsampling yields different distributions each. This enables to ensure the stability of the procedure, to define the errors bars and to decrease the influence of outliers, if any. The specific choice of parameters – the 80% subsampling and the 5×5 repetitions – are selected to adequately represent the distributions for comparison, while avoiding both over-averaging and undersampling.

$$f_\beta(x) = \frac{1}{2\alpha\Gamma(1/\beta)} e^{(-\frac{|x-\mu|}{\alpha})^\beta} \quad (8)$$

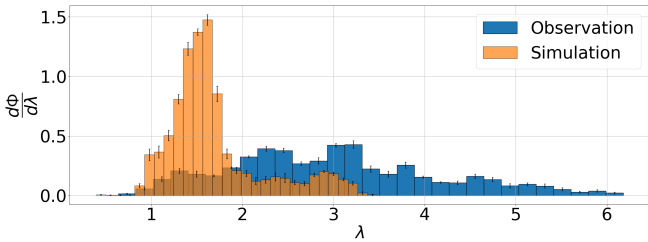
$$\alpha = \sqrt{\frac{\Gamma(1/\beta)}{\Gamma(3/\beta)}}; \quad \mu = 0$$



(a) J1022+1001

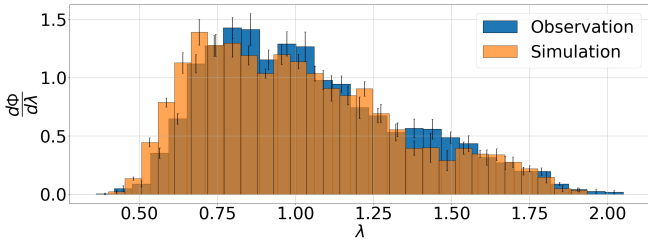


(b) J1125+7819

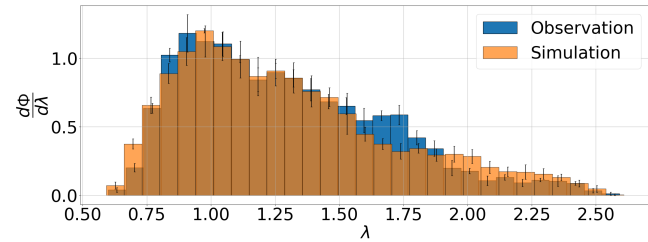


(c) J1903+0327

Fig. 1: The KSP distributions for the simulated/observed data of pulsars' white noise, when the histograms do differ. Orange and blue histograms correspond to simulations and observations, respectively.



(a) J1745+1017



(b) J1910+1256

Fig. 2: The same as in Figure 1, but for sample pulsars when the KSP distributions for the simulated/observed data are similar.

In (8) we have only a single free parameter β that describes the sharpness of the distribution. The scale parameter α is chosen such that the theoretical distribution has a unit variance. We consider two scenarios of data normalization and a choice of β . First, when β is a global parameter of a time series as described in 4.1, and second, where β is local and has a time dependence (4.2).

4.1. $\beta = \text{const}$

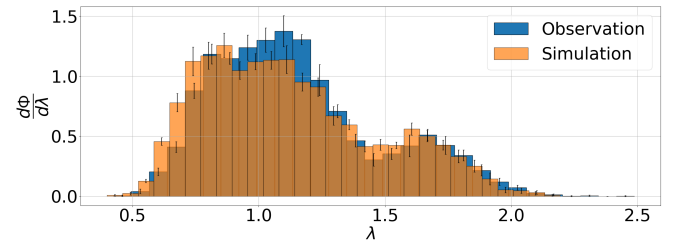


Fig. 3: The case of pulsar J1125+7819, when the KSP distributions became similar after introducing $\beta(t)$.

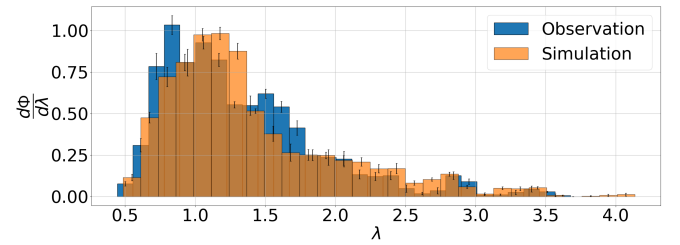


Fig. 4: The KSP distributions for pulsar J1910+1256. Introducing the time dependence in β does not significantly affect χ^2 .

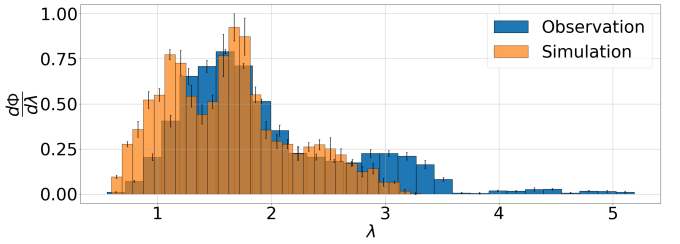


Fig. 5: The KSP distributions for the pulsar J1022+1001 after introducing the time dependence in β . Although $\langle\chi^2\rangle$ is smaller in the $\beta(t)$ approach (Tab. 2) than in the $\beta = \text{const}$ case (Tab. 1), they are of the same order.

Consider a time series of residuals of a pulsar, $\{R_i\}_{i=1}^N$ where N is the length of the series. We assume that they are identically distributed. In this scenario, we first normalize our series by subtracting the mean of the series \bar{R} and dividing by its standard deviation ΔR . Hence, we obtain normalized series $r_i = \frac{R_i - \bar{R}}{\Delta R}$.

We have performed this procedure on observed and simulated data using PINT (Luo, et al 2019, 2021; Susobhanan, et al 2024). Simulations use the same models, and the parameters

within them are used to extract residuals from the TOA. We observe that some of the pulsars' KSP distributions are not similar Fig. 1, while for others they are Fig. 2.

For a quantitative picture, we create 5 epochs of simulations for each pulsar presented, and calculate the reduced- χ^2 of the KSP histograms between observed and simulated data. To calculate χ^2 , we linearly interpolate histogram values and their corresponding errors into the same bins. Table 1 shows the minimum, maximum, mean, median, and standard deviation of χ^2 for each pulsar. Thus, the key point of our analysis is that the same numerical scheme is performed both for the data of observations and simulations.

4.2. $\beta = \beta(t)$

Now we assume that the properties of the distribution may change over time, hence β has a time dependence. We calculate β around each residual using maximum likelihood estimation. The algorithm for finding β_i for a residual time series R_i is the following:

1. We weight each residual value by weight

$$w_{ik} \propto \exp\left[-\frac{1}{2}\left(\frac{t_k - t_i}{h}\right)^2\right], \quad k = \overline{1; N}$$

where t_i, t_k are the time moments for R_i and R_k respectively, and h is a hyperparameter that is chosen via cross-validation.

2. We calculate the weighted mean and standard deviation and obtain normalized time-series for each time moment t_i : $r_{ik} = \frac{R_k - \bar{R}_i}{\Delta R_i}$.
3. We estimate β_i as:

$$\beta_i = \underset{\beta}{\operatorname{argmin}} \left[- \sum_k w_{ik} \log f_{\beta}(r_{ik}) \right]$$

| | $\min(\chi^2)$ | $\max(\chi^2)$ | $\text{med}(\chi^2)$ | $\langle \chi^2 \rangle$ | $\sigma(\chi^2)$ |
|------------|----------------|----------------|----------------------|--------------------------|------------------|
| J1022+1001 | 64 | 110 | 102 | 92 | 18 |
| J1125+7819 | 40 | 150 | 70 | 80 | 40 |
| J1745+1017 | 2.7 | 7.8 | 4.4 | 4.5 | 1.8 |
| J1802-2124 | 52 | 86 | 72 | 71 | 12 |
| J1832-0836 | 2 | 8 | 5 | 5 | 2 |
| J1903+0327 | 68 | 112 | 78 | 84 | 15 |
| J1910+1256 | 2 | 20 | 5 | 8 | 7 |
| J1918-0642 | 5.3 | 7.6 | 6.4 | 6.4 | 0.8 |
| J2043+1711 | 4 | 17 | 6 | 8 | 5 |
| J2317+1439 | 36 | 73 | 48 | 51 | 14 |

Table 1: Reduced- χ^2 data for each pulsar for $\beta = \text{const.}$

The following procedure of calculating the KSP histogram is the same, with the exception that now we normalize the distribution inside the sliding window similarly to the Section 4.1, i.e. without the weights. Table 2 shows the χ^2 values for this scenario.

Figures (3, 4, 5) illustrate examples of three differentiable cases: non-similar distributions became similar; similar and non-similar KSP distributions remained as they were.

5. Conclusions

We analyzed NANOGrav pulsar timing data using Kolmogorov's method. Namely, we concentrated on the white-noise

| | $\min(\chi^2)$ | $\max(\chi^2)$ | $\text{med}(\chi^2)$ | $\langle \chi^2 \rangle$ | $\sigma(\chi^2)$ |
|------------|----------------|----------------|----------------------|--------------------------|------------------|
| J1022+1001 | 21 | 60 | 32 | 36 | 13 |
| J1125+7819 | 2 | 14 | 8 | 7 | 4 |
| J1745+1017 | 5 | 30 | 11 | 13 | 8 |
| J1802-2124 | 30 | 90 | 60 | 60 | 20 |
| J1832-0836 | 2 | 9 | 5 | 5 | 2 |
| J1903+0327 | 18 | 54 | 43 | 41 | 12 |
| J1910+1256 | 5 | 19 | 7 | 10 | 5 |
| J1918-0642 | 6 | 23 | 16 | 15 | 6 |
| J2043+1711 | 5 | 15 | 11 | 10 | 3 |
| J2317+1439 | 12 | 26 | 14 | 18 | 6 |

Table 2: The same as in Table 1, for $\beta = \beta(t)$.

component of the observations, as it is the remainder after subtracting the known physical contributions from the TOAs. Comparing the observed white noise with simulated white noise, using the Kolmogorov stochasticity parameter of the signal as a metric, enables us the probing the possible physical components in the TOAs. These physical components may be deterministic, and thus being included in the timing models, or stochastic, as part of the red-noise (e.g., the GWB). The analysis is performed blindly with the same algorithm applied to all pulsars considered.

Assuming a generalized normal distribution — with a single free β parameter describing the sharpness of the distribution — as the underlying distribution for the white noise, we find both cases, when the white noise stochasticity agrees between observations and simulations and cases where it does not. The introducing of a time-dependent $\beta(t)$ improves the similarity, however, there remain instances in which the observational and simulated stochasticity still disagree. This can indicate the existence of non-stationary physical processes influencing the pulsar timing.

The KSP method can be used to test different models affecting pulsar timing, including e.g. modified theories of gravity or models for the dark sector of the universe (e.g. (Gurzadyan, et al 2023, 2025, 2026)). Namely, then the task will be to reproduce TOAs with the observed KSP properties, especially, at availability of higher precision and more amount of observational data.

Acknowledgements. We are thankful to the referee for many valuable comments. We acknowledge the use of The NANOGrav 15-Year Data Set; <https://zenodo.org/records/16051178> and ASCL Code Record of Astrophysics Source Code Library ASCL.net; ascl:1902.007.

References

- Agarwal N., et al, 2025, arXiv:2508.16534
- Agazie G. et al. (NANOGrav), 2023a, ApJ Lett. 951, L8
- Agazie G. et al. (NANOGrav), 2023b, ApJ Lett. 951, L9
- Agazie G. et al. (NANOGrav), 2025, arXiv:2510.16668
- Arnold V.I., 2008a, Nonlinearity, 21, T109.
- Arnold V.I., 2008b, Uspekhi Mat.Nauk, 63, 5
- Arnold V.I., 2008c, IC/2008/001, ICTP, Trieste
- Arnold V.I., 2009a, Trans. Moscow Math. Soc., 70, 31
- Arnold V.I., 2009b, Funct. An. Other Math. 2, 139
- Atto A.M., Berthoumieu Y., Megret R., 2013, Entropy, 15, 4782
- Ben-Dayan I., et al, arXiv:2508.15134
- Barenboim G., Ireland A., Stebbins A., arXiv:2511.13866
- Fiscella S.V.S., et al, 2025, arXiv:2509.21203
- Galikyan N., Kocharyan A.A., Gurzadyan V.G., 2025, A&A, 696, L21
- Gurzadyan V.G., 1999, EPL, 46, 114
- Gurzadyan V.G. and Kocharyan A.A., 2008, A&A 492, L33
- Gurzadyan V.G., et al, 2009, A&A, 497, 343
- Gurzadyan V.G., et al, 2010, EPL, 91, 19001
- Gurzadyan V.G., Durret F., 2011, EPL, 95, 69001

Gurzadyan V.G., et al, 2011, EPL, 95, 19001
Gurzadyan V.G., et al, 2014, A&A 566, A135
Gurzadyan V.G., et al, 2015, Roy.Soc. Open Sci., 2, 150143
Gurzadyan V.G., et al, 2023, A&A, 677, A161
Gurzadyan V.G., et al, 2025, A&A, 694, A252
Gurzadyan V.G., et al, 2026, A&A, 705, A70
Hoffman C., et al, 2023, PNAS, 120, e2218245120
Kolmogorov A.N., 1933, G.Ist.Ital.Attuari 4, 83
Lam M.T. et al, 2025, arXiv:2506.03597
Luo, J., et al, 2019, Astrophysics Source Code Library, record ascl:1902.007
Luo, J., et al, 2021, ApJ, 911, 45
NANOGrav Collaboration, 2025, Zenodo, doi:10.5281/zenodo.16051178
Sesana A., Vecchio A., Colacino C.N., 2008, MNRAS 390, 192
Sesana A., Figueira D.G., 2025, arXiv:2512.18822
Smith D.A. et al, 2023, ApJ, 958, 191
Szapudi I. et al, 2015, MNRAS, 450, 11
Susobhanan, A., et al, 2024, ApJ, 971, 150
Tiruvaskar S., Gordon C., arXiv:2506.18153